INTERNATIONAL JOURNAL OF CLIMATOLOGY
Int. J. Climatol. **34**: 2320–2329 (2014)
Published online 18 October 2013 in Wiley Online Library
(wileyonlinelibrary.com) DOI: 10.1002/joc.3841

RMetS
Royal Meteorological Society

An improved sea level forecasting scheme for hazards management in the US-affiliated Pacific Islands

Md. Rashed Chowdhury,[a]* Pao-Shin Chu[b] and Charles Chip Guard[c]

[a] *Pacific ENSO Applications Climate Center, Joint Institute for Marine and Atmospheric Research, University of Hawaii at Manoa, Honolulu, HI, USA*

[b] *Department of Meteorology, School of Ocean and Earth Science and Technology (SOEST), University of Hawaii at Manoa, Honolulu, HI, USA*

[c] *National Oceanic and Atmospheric Administration, National Weather Service, Weather Forecast Office, Guam, USA*

ABSTRACT: This study describes an improved seasonal sea level forecasting scheme by the Pacific ENSO Applications Climate Center (PEAC). Since 2005, an operational sea level forecasting scheme (3–5 months in advance) for the US-affiliated Pacific Islands (USAPI) has been instrumental (http://www.prh.noaa.gov/peac/sea-level.php). The El Niño-Southern Oscillation (ENSO) climate cycle and the sea-surface temperatures (SSTs) in the tropical Pacific Ocean are taken as the primary factors in modulating these forecasts on seasonal time scales. The current SST-based canonical correlations analysis (CCA) hindcast forecasts have been found to be skillful. However, the skill gradually decreases as the lead-time increases. This has motivated us to revisit the forecasting scheme at PEAC. In contrast to previous endeavours which relied only on SSTs, we now incorporate both trade winds and SSTs for modulating sea level variability on seasonal time scales.

The average forecasts for zero to three seasons' lead-times are found to be 0.647, 0.598, and 0.625 for combined SST and the zonal component of the trade wind (U), SST, and wind (U), respectively. It is therefore revealed that the combined SST-wind-based forecasts are more skillful than the SST or wind-based forecasts alone. It is particularly more efficient on longer time scales for most of the stations (e.g. 10–25% improvement on two to three seasons' lead-times). The improvements of these forecasts have enabled the capability of our clients in the USAPI region to develop a more efficient long-term response plan for hazard management.

KEY WORDS sea level; sea-surface temperature; trade wind; canonical correlation analysis; US-affiliated Pacific Islands

Received 15 November 2012; Revised 3 September 2013; Accepted 12 September 2013

1. Introduction

This study describes an enhancement of the sea level forecasting scheme by the Pacific ENSO Applications Climate Center (PEAC) on zero to three seasons (i.e. 3–12 months) lead-time. Currently based on the sea-surface temperatures (SSTs) in the tropical Pacific Ocean, PEAC runs a canonical correlation analysis (CCA) statistical model to generate sea level forecasts for the US-affiliated Pacific Islands (USAPI) with lead times of several months or longer (Chowdhury *et al.*, 2007b). On the basis of the hypothesis that El Niño-Southern Oscillation (ENSO) has a significant impact on the climate variability in the Pacific islands (i.e. Bjerknes, 1966, 1969; Ropelewski and Halpert, 1987; Chu 1995; Chu and Chen 2005; Barnston and He 1996; Yu *et al.*, 1997; McPhaden *et al.*, 2006; also see references therein), the ENSO climate cycle and the associated SSTs in the tropical Pacific Ocean are taken as the primary factors in modulating sea level variability on seasonal time scales. The co-variability between the tropical Pacific SST and sea level has also been used to construct a statistical Markov model (Xue and Leetmaa, 2000) where it has been shown that tropical sea level can be forecast with a moderate forecast skill due to predictability of ENSO (also see Xue *et al*., 2000).

The USAPI communities [i.e. Guam, Saipan, Palau (Malakal Harbor), Republic of the Marshall Islands (RMI) (Majuro, Kwajalein), Federated States of Micronesia (FSM) (the States of Chuuk, Kosrae, Pohnpei, and Yap) and American Samoa (Pago Pago) (Figure 1)] are most vulnerable to climate variability and change (Shea *et al.*, 2001), with low sea level during El Niño years and high sea level during La Niña years (Chowdhury *et al.*, 2007a). Because of this ENSO-related fluctuation of sea level, there has been a demand for advance information on sea level variability on month-to-seasonal time scales. The PEAC Center produces the real time sea level forecasts and publishes them at the official web site of PEAC (http://www.prh.noaa.gov/peac/sea-level.php). This information has also been distributed through the appropriate channels (e.g. printed Quarterly issue of the *Pacific ENSO Update* newsletter) to the right stakeholders (see Schroeder *et al.*, 2012 for an extensive review of PEAC's activities on climate forecasting, warning, and response activities).

* Correspondence to: Dr Md. R. Chowdhury, Principal Research Scientist, Pacific ENSO Applications Climate Center, University of Hawaii at Manoa, 2525 Correa Road, HIG 350, Honolulu, HI 96822, USA. E-mail: rashed@hawaii.edu

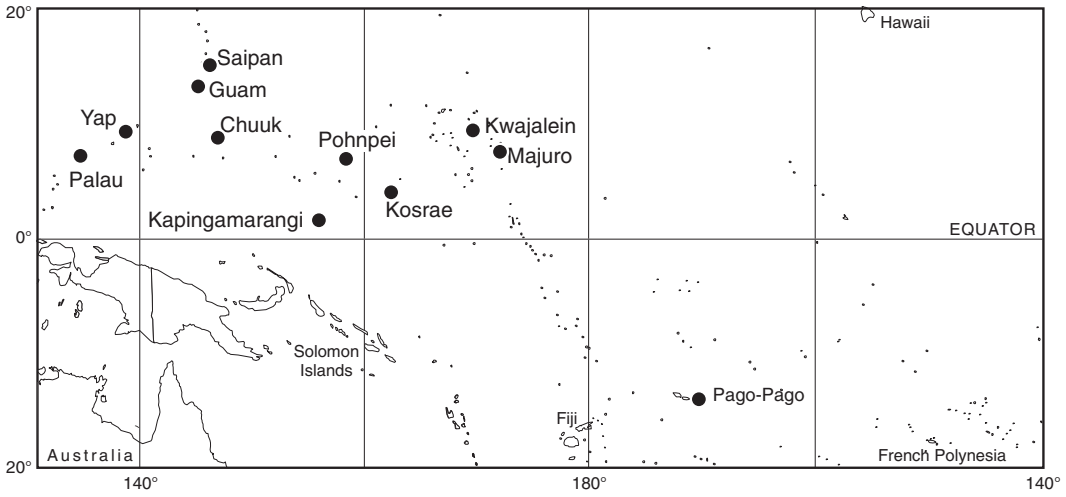

Figure 1. Locations of US-affiliated Pacific Islands–that are studied are labelled with black dots (note that because of lack of data, the atoll Kapingamarangi was finally dropped from the analysis).

While the 3–5 months forecasts have served our clients very well over the years, the demand for longer lead time (e.g. 6–12 months) forecasts has increased considerably for the support of long-term planning and management in climate-sensitive sectors such as water resources, fisheries and aquaculture, agriculture, emergency management, utilities, and coastal zones. This is the primary consideration that motivated us to revisit the current sea level forecasting scheme at PEAC. In addition, the pronounced sea level rise at several locations in the USAPI region during the La Niña years of 2007–2008 (Chowdhury *et al.*, 2010) also motivated us to explore the role of the trade winds in this recent rise. While seasonal variations in sea level can partly be caused by seasonal changes in wind, the recent trend of enhanced trade winds in the western tropical Pacific (WTP) (Lee and McPhaden, 2008; Feng *et al.*, 2010; Timmermann *et al.*, 2010; Merrifield, 2011; Merrifield and Maltrud, 2011; L'Heureux *et al.*, 2013; Newman, 2013) may be considered as one of the possible explanations for this rise. Tide gauge records indicate that the current high sea level trends in the WTP represent a significant shift in trend since the early 1990s as compared with the previous 40 years (Merrifield, 2011). Merrifield and Maltrud (2011) attributed the rise to a multidecadal increase in the Pacific trade winds, similar to, but distinct from, wind-driven La Niña events on inter-annual timescales. It is speculated that the Pacific trade wind enhancement since the early 1990s is fuelled by an increase in latent heat content in a warming atmosphere, which invigorates deep convection in the tropics and speeds up the atmospheric circulation. This generally supports the notion of a strengthening Hadley circulation in recent decades (Chen *et al.*, 2002; Mitas and Clement, 2005).

Whether these enhanced trade winds are a short-term anomaly or a longer-term trend remains an open question. For example, based on National Centers for Environmental Prediction (NCEP)/National Center for Atmospheric Research (NCAR) reanalysis II records, Garza *et al.* (2012) noted that changes in trade wind strength over the WTP (150°E to the Dateline) are small over the last three decades. Nevertheless, there is a clear indication that, in addition to thermal expansion, the trade wind is one of the major driving forces for sea level variations in the USAPI region. As a result, the current SST-based CCA forecasts at PEAC are found to be less efficient in capturing the seasonal sea level variability for the USAPI region; this is particularly true when the lead-time increases to two to three seasons. Therefore, in addition to SST, the recent trend of trade winds is hypothesized to be a contributing factor for seasonal sea level variability on month-to-seasonal time scales. The contributions by the trade winds have been thoroughly examined to determine the possibilities of improvement of the current operational forecasting schemes at PEAC. The final result is aimed at providing more skillful, longer-term seasonal sea level outlooks for the USAPI region.

This article is organized in the following manner. Section 2 describes the data procurement process and a brief description of the research methodology. Research results and discussions are located in Section 3 and the concluding remarks are presented in Section 4.

2. Data and research methodology

The research-quality sea-level data from the University of Hawaii Sea level Center (UHSLC) are used in this study. NCEP/NCAR historical monthly fields of the global SST and zonal wind (U) at 850-hPa are also used. Consistent with the current climatology of sea level records, the record starting from January 1975 to December 2010 is used. The methodology is comprised of composite analyses of seasonal variations of SST and zonal winds, linear correlation of SST and wind (henceforth, wind or zonal wind synonymously used) with sea level, empirical

Table 1. Percent of variance explained by eigenvectors (Ek/SST-Wind) for the Pacific sea-surface temperatures and winds (values in parentheses are cumulative variance by the k largest eigenvalues).

Ek/SST-Wind	JFM	AMJ	JAS	OND
E1	27.0 (27.0)	18.5 (18.5)	27.0 (27.0)	27.5 (27.5)
E2	12.0 (39.0)	13.0 (31.5)	12.0 (39.0)	12.0 (39.5)
E3	8.0 (47.0)	10.0 (41.5)	8.5 (47.5)	6.5 (46.0)
E4	6.0 (53.0)	6.5 (48.0)	6.5 (54.0)	6.0 (52.0)
E5	5.0 (58.0)	6.0 (54.0)	4.0 (58.0)	4.0 (56.0)
E6	4.0 (62.0)	5.0 (59.0)	3.8 (61.8)	3.5 (59.5)
E7	3.8 (65.8)	4.0 (63.0)	3.6 (65.4)	3.0 (62.5)
E8	3.0 (68.8)	3.0 (66.0)	3.0 (68.4)	2.5 (65.0)

AMJ, April–May–June; JAS, July–August–September; JFM, January–February–March; OND, October–November–December.

Table 2. Percent of variance explained by eigenvectors (Ek/sea level) for sea levels (values in parentheses are cumulative variance by the k largest eigenvalues).

Ek/sea level	JFM sea level	AMJ sea level	JAS sea level	OND sea level
E1	55.0 (55.0)	65.0 (65.0)	76.0 (76.0)	74.0 (74.0)
E2	18.0 (73.0)	16.0 (81.0)	13.0 (89.0)	12.0 (86.0)
E3	15.0 (88.0)	8.0 (89.0)	5.0 (94.0)	8.0 (94.0)

AMJ, April–May–June; JAS, July–August–September; JFM, January–February–March; OND, October–November–December.

orthogonal function (EOF) analysis, and CCA methods (e.g. Stone, 1974; Chu and He, 1994) to forecast sea level on seasonal time scales.

In the combined EOF analysis, the SST and zonal wind (U) fields are weighted equally. The EOF analyses of the SST data were carried out to minimize problems of collinearity and generate independent, contiguous SST and wind indices. Leading EOFs are selected as independent variables for the subsequent CCA model. The leading EOFs of SST and wind anomalies (X-EOFs) were calculated for each season. Other than the first three modes, the hindcast skill is less sensitive to the number of EOFs retained. In our analyses, a total of eight eigenmodes were chosen for the SST and U in the CCA model and the optimal numbers of EOFs (maximum five) were retained based on the cross-validated skill (goodness index) (Table 1). The EOFs for SST and wind analysis explained 65–69% of the total variance (Table 1) and the EOFs for sea levels (Y-EOFs) provided 88–94% of the total variance, with the first three modes retained (Table 2). The percent of variance explained in April–May–June (AMJ) SST (X-EOFs) is 18.5, which is relatively weak as compared with other seasons (Table 1). One possible reason for this weak variance could be related to the effect of the spring predictability barrier due to the interaction between SST and wind that might have eroded the signal of hindcast. Therefore, the leading modes did not account for the large percentages of variance. The signal is spread among the first few modes instead of being concentrated in the major leading one. For example, in this case, SST EOF3 for AMJ explained 10% of the variance, which is higher than the corresponding values for all other seasons' EOF3 (Table 1).

CCA analysis is performed to identify the optimal coupled anomaly pattern relationship between local and large-scale spatial patterns. This analysis has been found to be a popular statistical method for climate forecasts on month-to-seasonal time scales (e.g. Barnett and Preisendorfer, 1987; Chu and He, 1994; Barnston and He, 1996; Cherry, 1996; Yu *et al.*, 1997). CCA analysis allowed us to investigate the relationship between *two sets* of basis vectors, one for x and the other for y such that the correlation between the *projections* of the variables onto these basis vectors are mutually maximized. In this case, the basic vectors are SST and winds (x) and sea level (y). The hindcast skill of the CCA model for 1975–2011 is estimated using a cross-validated scheme with 1 year withheld. Auto-correlations in the sea-level data are generally found to be small (<0.1) and withholding 1 year is justified for low auto-correlations. Therefore all available data were used except those data for the season for which the prediction was targeted. The climatology is recomputed and the anomaly of the target year is redefined in terms of the means of the other years (since January 2013, forecasts are prepared based on 1983–2001 climatology). By doing this repeatedly, we obtain 36 forecasts of sea level, which were compared with the observed sea level. The Climate Predictability Tool (CPT) software (available at http://iri.columbia.edu/outreach/software/) was used to generate CCA hindcast results.

3. Results and discussions

3.1. EOF analysis of SST, wind, and sea-level records

The principal loading patterns of SST and U anomalies for EOF1 and EOF2 are presented in Figures 2 and 3, and the time-dependent coefficient of the combined SST and U is shown in Figure 4. The corresponding canonical component time-series are shown in Figure 5. The spatial pattern of X-EOF1 for SST (X Spatial Loadings: Mode 1) (Figure 2) resembles those of the leading eigenmodes presented in past studies (e.g. Kawamura, 1994 and references therein). For X-EOF1, which described aspects of ENSO, negative loadings exist over the tropical western Pacific extending to the subtropical latitudes, and large positive loadings exist over the central and eastern equatorial Pacific (Figure 2, left panel). In this mode EOF1, the large positive loadings over the central and eastern equatorial Pacific and relatively weak loading in the tropical Indian Ocean (not shown in Figure 2) resemble slightly different features from other similar studies (e.g. Hsiung and Newell 1983; Nitta and Yamada, 1989). Furthermore, it can also be seen in this mode that negative loadings over the central North

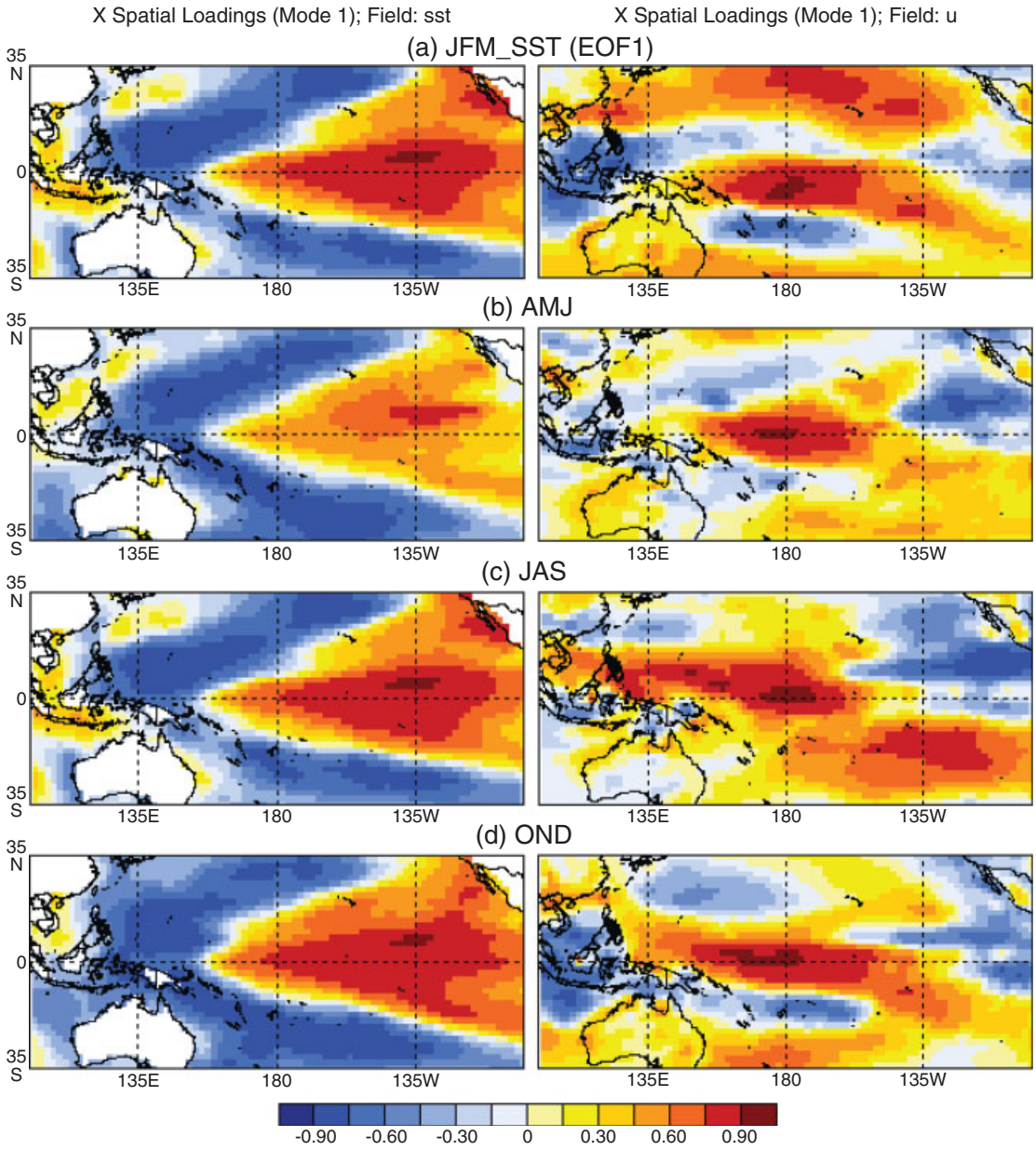

Figure 2. The principal loading patterns of SST (left panel) and U (right panel) anomalies for EOF1 (latitude 35°N–35°S, longitude 100°E–100°W).

Pacific around 20°–30°N are not very dominant, particularly for July–August–September (JAS). Thus, it is concluded that this mode accounts for the fundamental SST fluctuations over the equatorial Pacific and is not very strongly linked to those over the tropical Indian Ocean or the central North Pacific, as in Kawamura (1994). The spatial pattern of EOF2 for SST (X Spatial Loadings: Mode 2) (Figure 3, left panel) shows some noteworthy differences to that of the corresponding EOF1 (Figure 2) and EOF3 (not shown). In EOF2 (Figure 3(a)–(c), left panel), large positive loadings are located over the western Pacific and the South China Sea, whereas negative loadings exist in the mid-latitude of the North Pacific. Also, weak positive loadings exist in low-latitude regions of the eastern and central Pacific.

X-EOF1 for the zonal wind component (U) (Figure 2, right panel) is associated with an enhanced divergence anomaly over the Maritime Continent. This is reflected by the lower tropospheric easterly wind anomalies across the Indian Ocean and Maritime Continent and westerly anomalies over the equatorial central Pacific (note the sign in EOF patterns is arbitrary). EOF2 (Figure 3, right panel) is associated with enhanced convergence across the tropical Pacific Ocean. Lower tropospheric westerly (easterly) zonal wind anomalies are found across the eastern Maritime Continent and western Pacific Ocean (Central Pacific Ocean). One notable observation is that while both the EOF1 and EOF2 described aspects of ENSO, the EOF2 in JAS and October–November–December (OND) are slightly different from those of January–February–March (JFM)

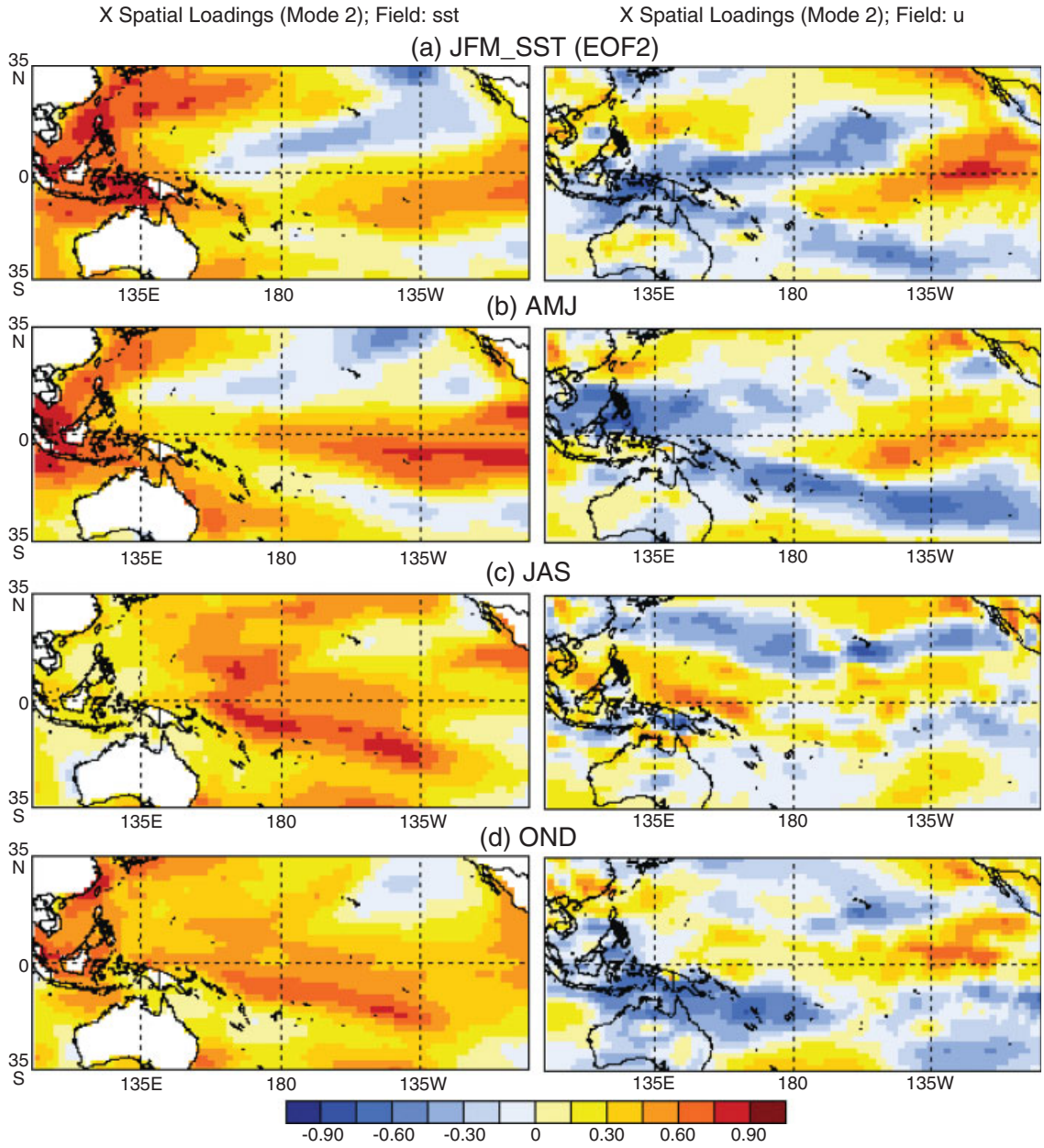

Figure 3. The principal loading patterns of SST (left panel) and U (right panel) anomalies for EOF2 (latitude 35°N–35°S, longitude 100°E–100°W).

and AMJ (Figure 3), which could be a reason why ENSO is much better defined in OND than in AMJ. EOF2 also shows a pattern of global warming (i.e. JAS and OND) as the weight is growing over time (Figure 4) (also see Trenberth and Stepaniak, 2001).

The temporal variability of EOF1 (for SST and U) coincides quite well with the occurrence of ENSO events having a quasi periodicity of 2–5 years (Figure 4). From the time-dependent EOF coefficients, major and moderate years of El Niño such as 1982–1983, 1997–1998, and 2009–2010 stand out. There is also an indication of interdecadal variability in the EOF1 time-series, particularly in AMJ and JAS SST modes. However, an expanded El Niño signal (well off the tropics) is visible in EOF1 (Figure 2) which could be a mixture of El Niño and Pacific Decadal Oscillation (PDO). The PDO is a basin-wide pattern of SST consisting of two phases, each commonly lasting 10–30 years (Mantua *et al.*, 1996). Moreover, the PDO signal is more evident in the mid latitude, in contrast to ENSO's tropical signal.

Time-series of eigenvector coefficients for the second mode is in contrast with that of EOF1 (Figure 4). For AMJ, JAS, and OND they exhibit a long-term upward trend with a pronounced signal in the last 20 years. Similar features have also been found in Kawamura (1994) and Allan and Slingo (2002). The SST EOFs in the current SST-U-based model and the previous SST-based model corresponded well, particularly in the western Pacific region; however, the only noteworthy difference observed is a cooling trend in the current modes over the

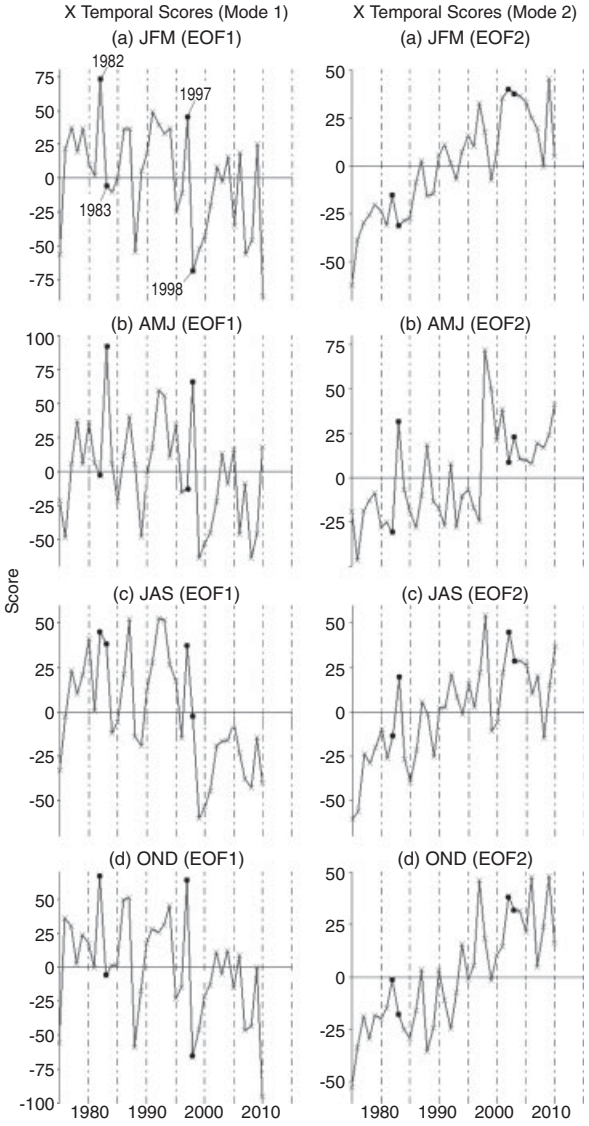

Figure 4. Time-dependent coefficients of the combined SST-U for EOF1 (left) and EOF2 (right).

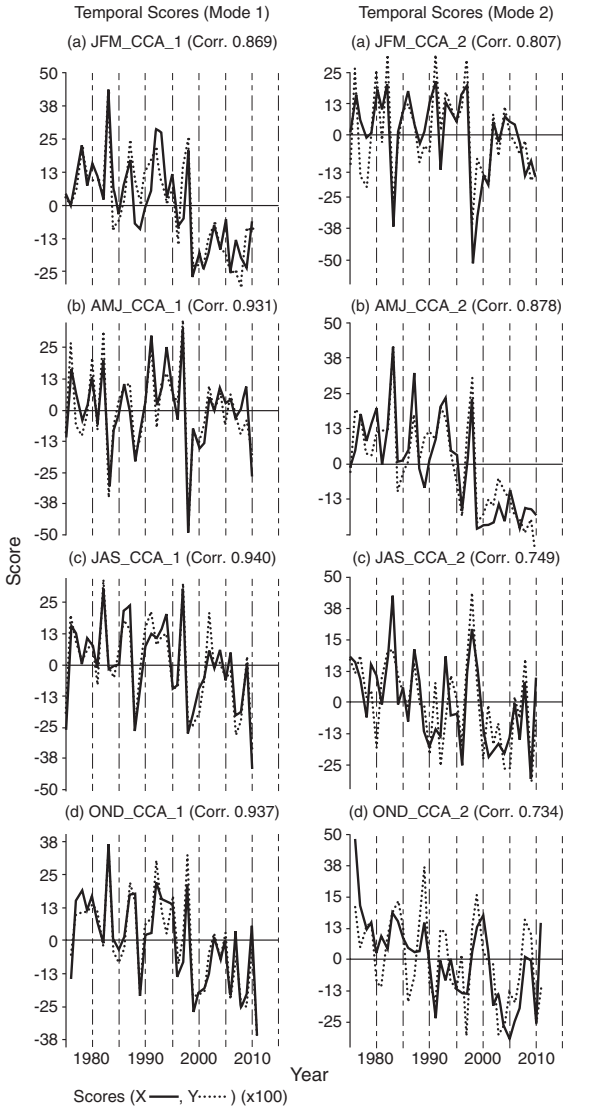

Figure 5. Links between CCA-X and CCA-Y (combined SST-U) for modes EOF1 (left) and EOF2 (right) [X (firm line) stands for SST and Y (dotted line) stands for sea level] (Canonical correlations are shown in parenthesis).

South China Sea in this study (Figures 2 and 3) (SST-only EOFs are not discussed in detail as they are available in Chowdhury *et al.*, 2007b).

3.2. CCA model forecast and hindcast skill

Table 3 provides SST-based cross-validation correlation skills for zero season lead forecasts for the USAPI stations. Table 4 provides the same analysis with the wind (U) component. To compare with our new forecasts scheme, Table 5 provides combined SST and wind-based (henceforth, SST-Wind or SST-U synonymously used) correlation skills also at zero season lead-time. Regardless of SST-, U-, or SST-U-based methods, sea level forecasts for all the four seasons are reasonably well predicted using the CCA model (Tables 3, 4, and 5). Out of the seven USAPI stations, the average skills of zero-season lead forecasts for six of the stations (i.e. except Pago Pago) are found to be above 0.644. Both the SST- and U-based forecasts are found to be equally skillful; however, some stations are shown to have better skill with the SST-only variable (i.e. Majuro, Pago Pago), while others tended to show better skill with the U variable (i.e. Guam, Malakal, Yap, Pohnpei, and Kwajalein). It is noteworthy that, as compared with SST- or U-based forecasts, the SST-U-based forecasts display improvements on the zero-season lead-time, particularly for Malakal, Majuro, and Pago Pago. The links between CCA-X (combining both SST and U) and CCA-Y for EOF1 and EOF2 are shown in Figure 5. Both of the time-series corresponded very well for all four seasons with canonical correlations greater than 0.869 for EOF1 and 0.743 for EOF2.

It is evident that there has been an improvement with the SST-U-based forecasts in all zero to three seasons' lead-times. It is also noteworthy that while at zero lead SST- and U-based forecasts are equally skillful, the skill level of U-based forecasts gradually increased relative to

Table 3. SST-based CCA cross-validation skill for four seasons (zero-season lead-time).

Predictor (SST) period	Target season (sea level)	Guam	Malakal	Yap	Pohnpei	Majuro	Kwajalein	Pago-Pago
JFM	AMJ	0.668	0.578	0.732	0.793	0.710	0.598	0.765
AMJ	JAS	0.617	0.715	0.627	0.684	0.631	0.450	0.786
JAS	OND	0.771	0.840	0.837	0.854	0.756	0.805	0.485
OND	JFM	0.797	0.808	0.781	0.831	0.705	0.722	0.754
Average		0.713	0.735	0.744	0.791	0.701	0.644	0.698

AMJ, April–May–June; JAS, July–August–September; JFM, January–February–March; OND, October–November–December. All values are significant at 1% level. Note that lead time is the time interval between the end of the initial period and the beginning of the forecast period. Also note that forecasts are thought to be of useful skill (or at least fair skill) if the CCA cross-validation value is greater than 0.3. Higher skills correspond to greater expected accuracy of the forecast.

the SST-based forecast as the number of leading seasons increased. This is an interesting finding that we would like to study further in the foreseeable future. At this stage, subsequent discussions are limited to the combined SST-U-based and SST-based forecasts only, the latter being the traditional sea level forecast approach.

Figure 6 shows average CCA cross-validation hindcast skills for four seasons (i.e. JFM, AMJ, JAS, and OND) for each of the USAPI stations at zero to three seasons' lead-times. The percentage of improvement is also shown by the dotted line. As indicated, different islands show different levels of predictive skill. As compared with SST-based forecasts, the SST-Wind-based forecasts displayed marginal to moderate improvements at zero season lead-time for all stations. At a one-season lead, besides showing a marginal improvement for Pohnpei, and a marginal decline for Pago Pago, all other stations displayed considerable improvements. At two- and three-season leads, the quality of forecasts improved considerably (e.g. 10–25%) for all stations, with the exception of Guam and Pago Pago at the two-season lead and Majuro at the three-season lead. It is noteworthy that the lone South Pacific Island, Pago Pago, did not show much improvement in the SST-U-based model. However,

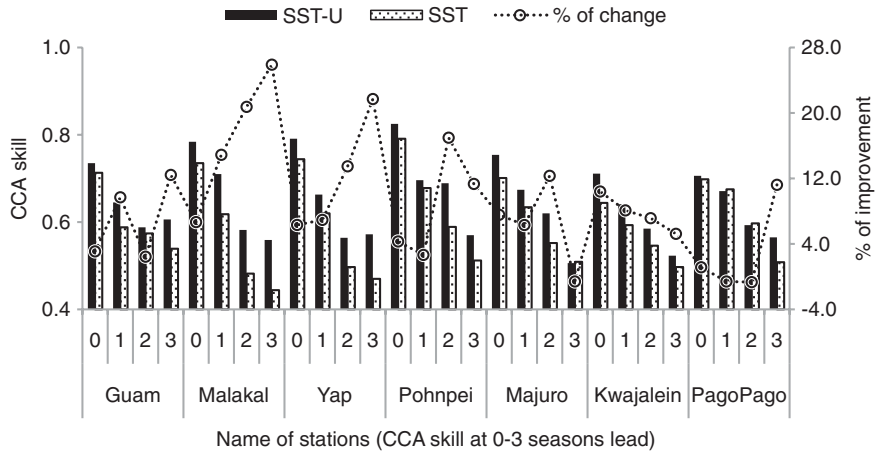

Figure 6. Average of four seasons (i.e. JFM, AMJ, JAS, and OND) forecast skills for each of the USAPI stations at zero to three seasons-lead. Note that the forecast at zero-season lead means that the 'sea level' of the target season (e.g. JFM) is simulated based on SST-U and SST of the previous season (e.g. OND, also see Tables 3–5). Similarly, one-, two-, and threee-season lead-time means sea level forecasts based on SST-U and SST of the previous JAS, AMJ, and JFM seasons. Percent of improvement is shown by the dotted line.

Table 4. Wind (U)-based CCA cross-validation skill for four seasons (zero-season lead-time).

Predictor (zonal wind) period	Target season (sea level)	Guam	Malakal	Yap	Pohnpei	Majuro	Kwajalein	Pago-Pago
JFM	AMJ	0.646	0.550	0.712	0.798	0.592	0.627	0.692
AMJ	JAS	0.683	0.833	0.848	0.868	0.710	0.804	0.562
JAS	OND	0.828	0.881	0.891	0.870	0.754	0.808	0.192
OND	JFM	0.792	0.821	0.849	0.855	0.668	0.802	0.669
Average		0.737	0.771	0.825	0.848	0.681	0.760	0.529

AMJ, April–May–June; JAS, July–August–September; JFM, January–February–March; OND, October–November–December. All values are significant at 1% level. Note that lead time is the time interval between the end of the initial period and the beginning of the forecast period. Also note that forecasts are thought to be of useful skill (or at least fair skill) if the CCA cross-validation value is greater than 0.3. Higher skills correspond to greater expected accuracy of the forecast.

Table 5. SST and wind (SST-U)-based CCA cross-validation skill for four seasons (zero-season lead-time).

Predictor (SST-Wind) period	Target season (sea level)	Guam	Malakal	Yap	Pohnpei	Majuro	Kwajalein	Pago-Pago
JFM	AMJ	0.669	0.625	0.735	0.761	0.755	0.654	0.789
AMJ	JAS	0.644	0.812	0.740	0.793	0.750	0.605	0.717
JAS	OND	0.819	0.880	0.887	0.885	0.775	0.830	0.558
OND	JFM	0.809	0.817	0.803	0.861	0.737	0.754	0.758
Average		0.735	0.784	0.791	0.825	0.754	0.711	0.706

AMJ, April–May–June; JAS, July–August–September; JFM, January–February–March; OND, October–November–December. All values are significant at 1% level. Note that lead time is the time interval between the end of the initial period and the beginning of the forecast period. Also note that forecasts are thought to be of useful skill (or at least fair skill) if the CCA cross-validation value is greater than 0.3. Higher skills correspond to greater expected accuracy of the forecast.

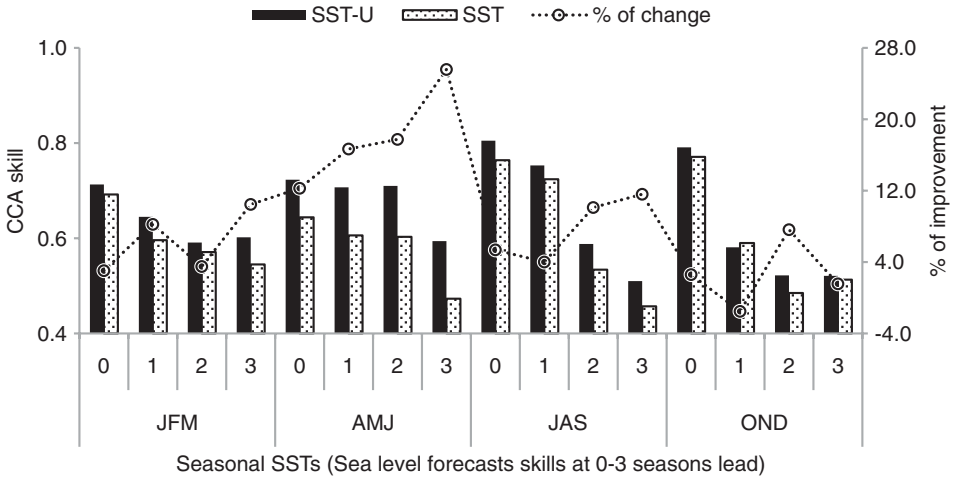

Figure 7. Average forecast skills for all seven USAPI stations for seasons JFM, AMJ, JAS, and OND at zero to three seasons-lead. Percent of improvement is shown by the dotted line.

at this stage, further diagnostic discussion on why the skill at longer lead-times has increased substantially in the combined SST-U-based model for all stations except Pago Pago is beyond the scope of this study.

On the basis of SST-Wind predictors, the average skill of zero to three seasons lead forecast for seasons JFM, AMJ, JAS, and OND are found to be 0.638, 0.684, 0.664, and 0.604, respectively (Figure 7). These forecasts are 6, 18, 7, and 2.5% higher than the similar SST-based forecasts. Among the four seasons, SST-Wind of AMJ and JAS exhibited the highest skill. AMJ provides 18 and 26% better forecasts on two- and three-season lead-time relative to the SST-based forecasts. JAS provides 10 and 12% improvement on the same seasonal time-scale. These results suggest that the addition of U in our model significantly improves the sea level predictability of AMJ and JAS on longer time-scales. For example, it can be stated here that the average JAS SST-based hindcast skill for two- and three-season lead (for AMJ and JAS seasons) are low (0.534 and 0.457, Figure 7). With the addition of U in the CCA model, the average skill has increased significantly to 0.588, 0.510, respectively, showing a 11 and 12% increase. Similarly, the addition of wind in the model also improved the OND SST-based forecast skill 8% for the JAS season (Figure 7). To show the improvement of hindcast skill in JAS, the observation and cross-validated hindcast time-series of sea level forecasts for Yap is shown in Figure 8. As compared with SST-based forecasting skill (0.335), the SST-U-based forecasting skill (0.496) displayed considerable improvement. Guam and Pohnpei also displayed similar improvements (not shown in Figure 8).

As compared with Chowdhury *et al.*, (2007b), where JAS displayed a weaker predictability that seemed to be an impact of the spring predictability barrier (Jin *et al.*, 2008), we observed an improved predictability here for the JAS season. The addition of the wind parameter in the model appears to reduce the impact of the spring predictability barrier and increases the hindcast skills considerably. While Yu *et al.*, (1997) found it to be very difficult to generate accurate rainfall forecasts for the USAPI using the spring SSTs as predictors, our current findings show that the combination of spring SST and wind do yield a higher skill for sea level forecasts for the USAPI region. The likely reason that JAS has better predictability is because ENSO responses are most pronounced during the boreal winter as the Pacific SST and surface pressure anomalies are more likely to be in phase and reach their peaks during the antecedent boreal winter/spring.

3.3. A synopsis of enhanced trade winds

The pronounced sea level rise in recent years can partly be attributed to the enhanced trade winds. A

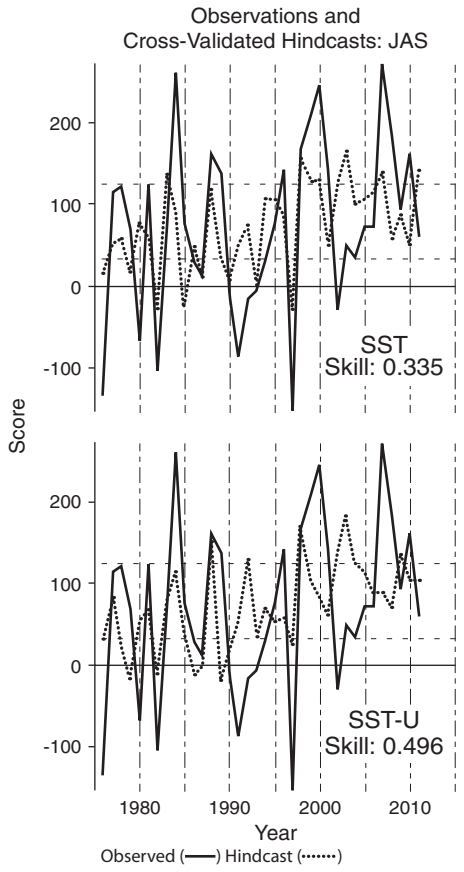

Figure 8. Observation (firm line) and cross-validated hindcast (dotted line) time-series for JAS sea level forecasts for Yap at three-seasons lead. SST-based results are shown in top panel (skill: 0.335) and SST-U-based results are shown in (bottom panel) (skill: 0.496).

determination of the underlying atmospheric and oceanic interactions responsible for the shift of this trend is beyond the scope of this study. Nevertheless, a review of available literature (Merrifield, 2011; Merrifield and Matrud, 2011 and references therein) provides a rich perspective on this issue. In studying the multidecadal increase of Pacific trade winds, Merrifield (2011) considered a number of possible connections, such as the dominant sea level trends associated with the timing and amplitude of interannual ENSO events over the short record, or with longer time-scale climate modes such as the PDO or the North Pacific Gyre Oscillation (NPGO) (Di Lorenzo *et al.*, 2008). From 1993 to 2001, the reconstruction indicates high rates of sea level rise in the western Pacific, similar to that shown by Church and White (2006). Merrifield (2011) concluded that the pattern reflects a shift from weak El Niño conditions early in the record to more La Niña conditions in 2001. Since then, the Pacific atmospheric and oceanic conditions have remained in a La Niña mode (Barnston 2012; pers. comm.).

Merrifield (2011) further added that the poor correspondence between sea levels and the PDO suggests that the primary wind anomalies associated with the PDO at decadal and interdecadal time scales are too far north to impact sea levels in the WTP and northeast Pacific (NEP) regions. However, as concluded, the positive phase of the NPGO corresponds to increased easterly trade winds, mid-latitude westerlies, and northerly winds in the NEP south of 40 N. These wind patterns contribute to a positive sea level anomaly response in the WTP and negative in the eastern tropical Pacific (ETP) and NEP via local forcing and longwave propagation, which matches the positive and negative correlations between the NPGO index and NEP and WTP sea levels, respectively (Merrifield, 2011).

4. Conclusions

The CCA model provides useful skill in predicting sea level in the Pacific Islands. The current SST-based CCA model forecasts (3–5 months lead-time) are well accepted by our clients at the USAPI region. However, the improved SST-Wind-based model forecasts produce more skillful products on the same time scales, particularly for the islands of Yap, Pohnpei, Majuro, Kwajalein, and American Samoa (Pago Pago) in the USAPI region. On 6–12 months lead-time, the SST-Wind-based forecasts provided more skillful results when compared with current SST-based forecasts. All stations showed considerable improvement. One plausible explanation for the success of adding the wind is the impact of ocean–atmosphere coupling. The SST alone may not always reflect this coupled mode. The SST reveals some of the sea level rise due to thermal expansion; the wind shows the surface stress contribution to sea level rise. With ENSO, the SST is usually present when the wind component is present, but the wind component is not always present when the SST is present. Therefore, the combination of SST and wind predictors offers additional advantages in sea level forecasting on longer time-scales.

While PEAC's current dissemination of sea level products is limited to 3–5 months lead-time, the improvement will enable PEAC to produce products with a 6–12 months lead-time. These products will specifically address a critical need of our clients: to more effectively conduct coastal hazards management in the USAPI region with the aid of longer, more accurate sea level predictions.

Acknowledgements

This project was funded by cooperative agreement NA17RJ1230 between the Joint Institute for Marine and Atmospheric Research (JIMAR) and the National Oceanic and Atmospheric Administration (NOAA). The views expressed herein are those of the authors and do not necessarily reflect the views of NOAA or any of its subdivisions. Special thanks are expressed to Mr Tony Barnston and Dr Mark Merrifield for reviewing an earlier version of this paper. Thanks are due to Drs John Marra and William Sweet for their valuable comments. We express our gratitude to the Sea Level Center (University of Hawaii) and the International

Research Institute for Climate and Society (IRI) for providing us easy access, manipulation, and visualization of earth science data. Grateful acknowledgements are expressed to the anonymous referees for careful reading and reviewing of this paper.

References

Allan RP, Slingo A. 2002. Can current climate forcings explain the spatial and temporal signatures of decadal OLR variation? *Geophys. Res. Lett.* **29**(7): 1–4.

Barnett TP, Preisendorfer R. 1987. Origins and levels of monthly and seasonal forecast skill for United States surface air temperatures determined by canonical correlation analysis. *Mon. Weather Rev.* **115**: 1825–1850.

Barnston AG, He Y. 1996. Skill of CCA forecasts of 3-month mean surface climate in Hawaii and Alaska. *J. Climate* **9**: 2020–2035.

Bjerknes J. 1966. A possible response of the atmospheric Hadley circulation to equatorial anomalies of ocean temperature. *Tellus* **18**: 820–829.

Bjerknes J. 1969. Atmospheric teleconnections from the equatorial Pacific. *Mon. Weather Rev.* **97**: 163–172.

Chen JY, Carlson BE, Del Genio AD. 2002. Evidence for strengthening of the tropical general circulation in the 1990s. *Science* **295**: 838–841.

Cherry S. 1996. Singular value decomposition analysis and canonical correlation analysis. *J. Climate* **9**: 2003–2009.

Chowdhury MR, Chu P-S, Schroeder T. 2007a. ENSO and seasonal sea-level variability – a diagnostic discussion for the U.S-affiliated Pacific Islands. *Theor. Appl. Climatol.* **88**: 213–224.

Chowdhury MR, Chu P-S, Schroeder T, Colasacco N. 2007b. Seasonal sea-level forecasts by canonical correlation analysis – an operational scheme for the U.S-affiliated Pacific Islands (USAPI). *Int. J. Climatol.* **27**: 1389–1402.

Chowdhury MR, Barnston AG, Guard C, Duncan S, Schroeder T, Chu P-S. 2010. Sea level variability and change in the U.S-Affiliated Pacific Islands – Understanding the high sea levels during 2006–08. *Weather* **65**(10): 263–268.

Chu P-S. 1995. Hawaii rainfall anomalies and El Nino. *J. Climate* **8**: 1697–1703.

Chu P-S, Chen H. 2005. Interannual and interdecadal rainfall variations in the Hawaiian Island. *J. Climate* **18**: 4796–4813.

Chu P-S, He Y. 1994. Long-range prediction of Hawaiian winter rainfall using canonical correlation analysis. *Int. J. Climatol.* **14**: 659–669.

Church JA, White NJ. 2006. A 20th-century acceleration in global sea level rise. *Geophys. Res. Lett.* **33**(L01602), DOI: 10.1029/2005GL024826.

Di Lorenzo E et al. 2008. North Pacific Gyre Oscillation links ocean climate and ecosystem change. *Geophys. Res. Lett.* **35**(L08607), DOI: 10.1029/2007GL032838.

Feng M, McPhaden MJ, Lee T. 2010. Decadal variability of the Pacific subtropical cells and their influence on the southeast Indian Ocean. *Geophys. Res. Lett.* **37**(L09): 606, DOI: 10.1029/2010GL042 796.

Garza JA, Chu P-S, Norton CW, Schroeder TA. 2012. Changes of the prevailing trade winds over the islands of Hawaii and the North Pacific. *J. Geophys. Res. (Atmospheres)* **117**: D 11109, DOI: 10. 1029/2011 JD 016888.

Hsiung J, Newell RE. 1983. The principal nonseasonal modes of variation of global sea surface temperature. *J. Phys. Oceanogr*. **13**, 1957–1967.

Jin EK *et al.* 2008. Current status of ENSO prediction skill in coupled ocean–atmosphere models. *Climate Dyn.* **31**: 647–664.

Kawamura R. 1994. A rotated analysis of global sea surface temperature variability with interannual and interdecadal Scales. *J. Phys. Oceanogr.* **24**: 707–715.

L'Heureux M, Lee S, Lyon B. 2013. Recent multidecadal strengthening of the Walker circulation across the tropical Pacific. *Nature Clim. Change* **3**: 571–576.

Lee T, McPhaden MJ. 2008. Decadal phase change in large-scale sea level and winds in the Indo-Pacific region at the end of the 20th century. *Geophys. Res. Lett.* **35**: L01605, DOI: 10.1029/2007 GL032419.

Mantua NJ, Hare SR, Zhang Y, Wallace JM, Francis RC. 1996. A Pacific interdecadal climate oscillation with impacts on salmon production. *Bull. Am. Meteorol. Soc.* **77**: 1275–1277.

McPhaden MJ, Zebiak SE, Glantz MH. 2006. ENSO as an integrating concept in Earth science. *Science* **314**: 1740–1745.

Merrifield MA. 2011. A shift in western tropical sea level during the 1990s. *J. Climate* **24**: 4126–4138.

Merrifield MA, Maltrud E. 2011. Regional sea level trends due to a Pacific trade wind intensification. *Geophys. Res. Lett.* **38**: L21605.

Mitas CM, Clement A. 2005. Has the Hadley cell been strengthening in recent decades? *Geophys. Res. Lett.* **32**: L03098, DOI: 10.1029/2004GL021765.

Newman M. 2013. Atmospheric science: winds of change. *Nature Clim. Change* **3**: 538–539.

Nitta T, Yamada S. 1989. Recent warning of tropical sea surface temperature and its relationship to the Northern Hemisphere circulation. *J. Meteor. Soc. Japan* **67**: 375–383.

Ropelewski CF, Halpert MS. 1987. Global and regional scale precipitation patterns associated with the El Niño–Southern Oscillation. *Mon. Weather Rev.* **115**: 1606–1626.

Schroeder TA, Chowdhury MR, Lander MA, Guard C, Felkley C, Duncan G. 2012. The role of the pacific ENSO Applications Climate Center in reducing vulnerability to climate hazards: experience from the U.S-affiliated Pacific Islands. *Bull. Am. Meteorol. Soc.* **93**(6): 1003–1015.

Shea EL, Dolcemascolo G, Anderson CL, Barnston A, Guard CP, Hamnett MP, Kubota ST, Lewis N, Loschnigg J, Meehl G. 2001. Preparing for a changing climate: the potential consequences of climate variability and change, Technical Report, East–west Center, 102.

Stone M. 1974. Cross-validatory choice and assessment of statistical predictors. *J. Roy. Stat. Soc.* **B36**: 111–147.

Timmermann A, McGregor S, Jin F-F. 2010. Wind effects on past and future regional sea level trends in the South Indo-Pacific. *J. Climate* **23**: 4429–4437.

Trenberth KE, Stepaniak DP. 2001. Indices of El Niño Evolution. *J. Climate* **14**: 1697–1701.

Xue Y, Leetmaa A. 2000. Forecast of tropical Pacific SST and sea level using a Markov model. *Geophys. Res. Lett.* **27**: 2701–2704.

Xue Y, Leetmaa A, Ji M. 2000. ENSO prediction with Markov models: The impact of sea level. *J. Climate* **13**: 849–871.

Yu Z-P, Chu P-S, Schroeder T. 1997. Predictive skills of seasonal to annual rainfall variations in the U. S. affiliated Pacific islands: Canonical correlation analysis and multivariate principal component regression approaches. *J. Climate* **10**: 2586–2599.

